

An Evaluation of Enhanced Cooling Techniques for High-Heat-Load Absorbers

S. Sharma, C. Doose, E. Rotela and A. Barcikowski

The Advanced Photon Source, Argonne National Laboratory, Argonne, IL

Phone: (630) 252-6820; Fax: (630) 252-5948

E-mail: sharma@aps.anl.gov

Abstract

Many components of the storage ring and front ends in the third generation of light sources are subjected to high heat loads from intense x-rays. Temperature rises and thermal stresses in these components must be kept within acceptable limits of critical heat flux and low-cycle fatigue failure. One of the design solutions is to improve heat transfer to the cooling water either by increasing water velocity in the cooling channels or by using inserts, such as porous media, twisted tapes and wire springs. In this paper we present experimental and analytical results to compare various enhanced cooling techniques for conditions specific to heating from an x-ray fan.

Keywords: heat transfer, high heat load, enhanced cooling, absorbers

1. Introduction

The Advanced Photon Source (APS) 7-GeV storage ring (SR) is presently operating at its Phase I current limit of 100 mA. Future goals for the APS include increasing the beam current to 200 mA over the next several years—eventually to the Phase II specification of 300 mA. Detailed analyses are underway to ensure the thermal safety of SR absorbers and new front-end and beamline components [1,2] at higher beam currents.

For existing components, the straightforward solution to handle higher heat loads would be to increase water velocities in their cooling channels. Previous analyses for the SR absorbers and scrapers showed that velocities of up to 15 ft/sec would be required at 300 mA. Water circuits for these components contain flow restrictors (orifices or small-diameter coiled tubes) that can be replaced to provide increased flow. We anticipate that in some circuits the required velocities would not be achieved even if the flow restrictors were completely removed. Erosion-corrosion of the cooling channels at higher velocities is also a serious concern.

A higher cooling efficiency can also be obtained by using turbulence-enhancing inserts in the cooling channels, such as wire meshes, twisted tapes and wire springs. Their effectiveness has been studied extensively under uniform heating conditions [3,4,5]. In this paper we present experimental and analytical results for such inserts, simulating concentrated heating from intense dipole x-rays. Practical matters that should be considered when implementing one of these enhanced cooling schemes are discussed.

2. Water Velocity Limits in Copper Channels

High water velocity in copper channels can strip the protective copper oxide layers and thus accelerate corrosion-erosion of the channels. The corrosion-erosion is a complex process involving, besides water velocity, other important parameters such as water chemistry (dissolved oxygen and pH), water temperature, component geometry, heat flux, radiation dose, and chemical composition of copper. For industrial and domestic copper piping installations, the recommended velocity is in the 5–8 ft/sec range [6,7]. This velocity range has often been adopted as a design criterion in some accelerator applications.

There is little experimental data in the literature supporting a bulk velocity limit of 8 ft/sec for oxygen-free copper in high-purity water. At Los Alamos National Laboratory (LANL), the specified design velocity for the LAMPF project was 15 ft/sec [8]. The LAMPF has been in service for 30 years with no components experiencing leaks operating within this velocity limit. A few leaks that were encountered after 25 years of service were attributed to a combination of higher water velocity (~25 ft/sec), brazed joints of poor design and manufacture, and poor quality of copper [8]. Similarly, the National Synchrotron Light Source has a few OFHC copper components operating in a 14-17 ft/sec range, and one component at 22.4 ft/sec [9] for about 20 years.

A set of three 3/8”(outer-diameter) OFHC copper tubes with several bends (Fig. 1) was installed in the APS SR tunnel in May 1998 to evaluate erosion-corrosion at high velocities. The nominal wall thickness of these tubes was 0.063”, but, in the bends, the outer walls reduced to 0.058”. Original flows in the three tubes were set at 2, 4 and 6 gpm with constant-flow (Griswald®) cartridges. Subsequently, however, pump impellers were reduced in size for the entire SR (to reduce vibration levels and supply-side pressures), which lowered flows in the tubes. When the tubes were removed from the tunnel in May 2002, the flow values were remeasured as 1.85, 3.43 and 4.89 gpm, respectively. The storage ring water is de-ionized to 7 megaOhm.cm and passes through 0.5 µm filters.



Fig. 1: OFHC copper tubes for erosion corrosion tests.

Table 1: Reduction in Wall Thicknesses for Different Flows

Flow gpm	Flow Ft/sec	Straight Thickness (in)	Bent Thickness (in)
1.85	12.1	0.063	0.058
3.43	22.4	0.063	0.057
4.89	32.0	0.063	0.057

Table 1 shows wall thickness values of both the straight and the bent parts of the tubes after four years of service. The wall thicknesses were measured with a Panametrics Model 25DL ultrasonic thickness gauge, which showed repeatability to within 0.001”

(maximum resolution 0.0001"). Six different readings were taken for both the straight and bent parts of the tubes. The readings, which were within 0.001" of each other, were averaged. As shown in the table, erosion-corrosion was not measurable for all flow velocities in the straight sections, or for the lower velocity of 12.1 ft/sec in the bends. For the latter case, erosion-corrosion was only about 0.001" after four years of service at 22.4 and 32.0 ft/sec.

An extensive literature search yielded almost no erosion-corrosion data for Glidcop [10] in high-purity water. From a short-time (582 hours) test at a high velocity of 41 ft/sec, Glidcop was shown to perform substantially better than OFHC copper [11]. At the APS, we are planning to do further erosion-corrosion tests on the OFHC copper tubes mentioned above and on 16 new Glidcop samples.

3. Experimental Setup

The experimental setup consisted of a water manifold with four parallel circuits with a copper heat-transfer block in each circuit (Fig. 2). Valves were installed to control the flow for each circuit. Each sample had one bore for the cooling water and four bores for electrical heater cartridges. A variety of inserts were used in the cooling bore to induce turbulent flow, namely, copper mesh, stainless-steel springs, and twisted stainless-steel tapes. The copper mesh is of standard APS design and fits inside a cooling bore diameter of 0.438". A narrow channel separated the hot and cold sides of the sample providing a concentrated heat load along the length of the sample. The two bores nearest the channel were equipped with four (two on each end) 500W heaters for a total of 2 kW heat load for all of the subsequent tests.

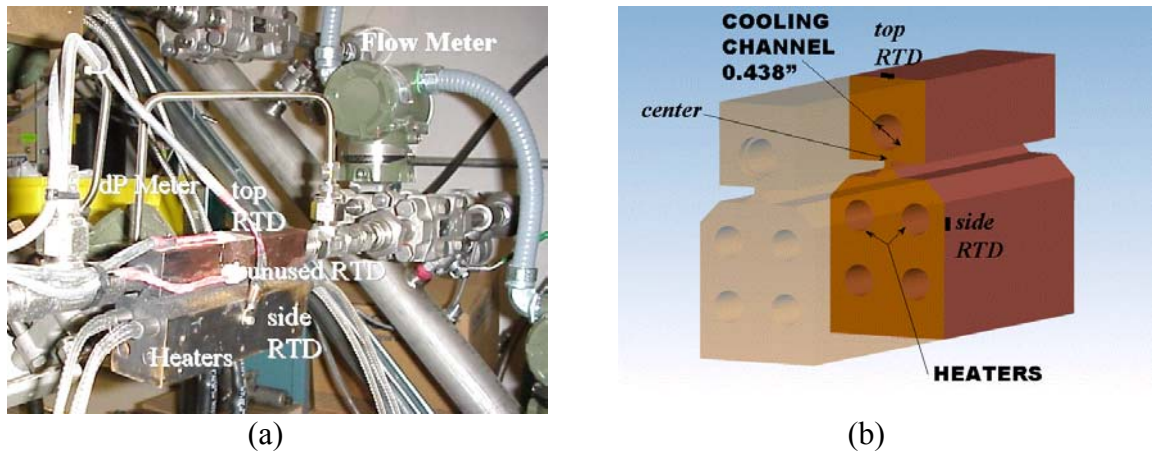


Fig. 2: Experimental setup for heat-transfer tests: (a) copper block and instrumentation, (b) cross-section showing channels and locations of the Omega Resistance Temperature Detectors (RTDs) .

For each sample, the water flows, differential pressures (dP), and temperatures were measured. The flows were measured using Yokagawa model EJA115 transducers. The dPs were measured using Yokagawa EJA110 transducers for the low dP circuits and using Viatron model 374 transducers for the high dP circuits. The Viatron transducers

had a range of 0-125 psi, and the repeatability was on the order of 1 to 2%. The Yokagawa dP transducers had a range of 0-14 psi, and the repeatability was on the order of 0.1%. The range of the flow meters was 0 to 6 gpm also with 0.1% repeatability.

The temperatures were measured on the *top* and *side* locations of the blocks, Fig. 2(b). Temperatures were also measured in the supply and return water lines using Omega Resistance Temperature Detectors (RTDs) with repeatability and resolution to 0.005°C. Bulk water temperature rise showed that only 3% of the heat input was convected to air. Twenty-five channels of data were collected (with a 5-½-digit resolution Keithley model 2700 data acquisition system) and saved to a PC.

4. Results for the Smooth-Bore Block

ANSYS finite element (FE) analyses were performed to determine temperature distributions inside the copper block with smooth bore. The heat transfer film coefficient, h_f , for the smooth bore was calculated by the Sieder-Tate equation [12]:

$$h_f = C (k/d) R_e^{0.8} P_r^{1/3} (\mu_b/\mu_w)^{0.14}, \quad (1)$$

where k = thermal conductivity of water, d = diameter of the channel, R_e = Reynolds number, P_r = Prandtl number, μ_b = fluid viscosity at bulk temperature, and μ_w = fluid viscosity at channel wall temperature. C is a constant, which is quoted variously between 0.019 to 0.027, with an average of 0.023. When the length-to-diameter ratio of the cooling channel is less than 60, a higher than average value is used to account for entrants effects. For FE analyses of the short channels of Fig. 2, we used $C = 0.025$, mainly because it gives a better correlation with the widely used Dittus-Boelter equation [13]. Average bulk water temperature rise is used to calculate R_e and P_r at different flows. Figure 3 shows plots of flow velocity, Reynolds number and film coefficient versus flow (gpm) at the reference temperature of 25°C.

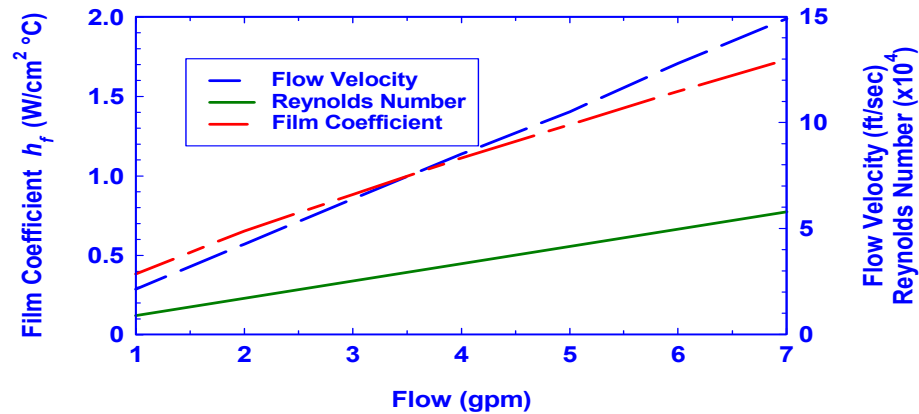
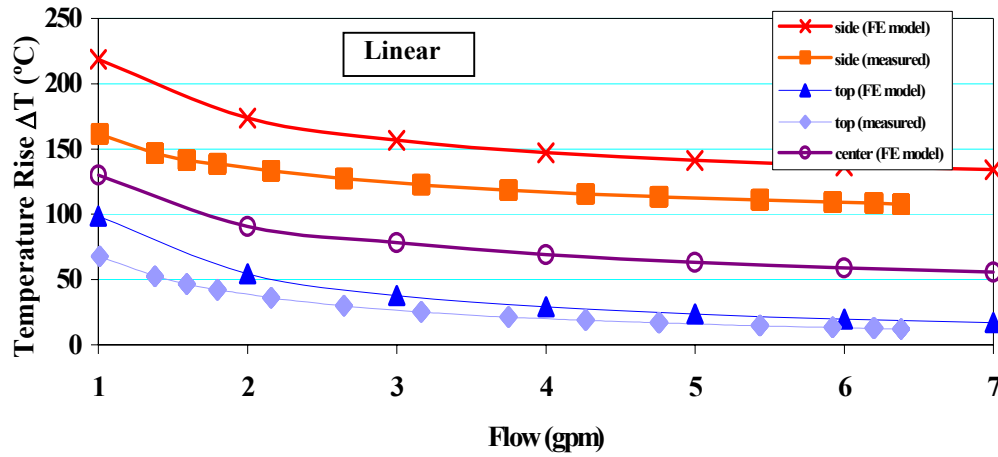


Fig. 3: Flow velocity, Reynolds number and film coefficient versus water flow in a 0.438"-diameter channel.

The film coefficient is assumed to be independent of wall temperature in linear FE analyses, i.e., the contribution of the viscosity factor, $(\mu_b/\mu_w)^{0.14}$, is ignored.

Temperatures at the *top* and *side* of the copper block, as well as at its *center* location, are plotted against flow in Fig. 4 (a). Only FE results are plotted for the *center* location (equivalent to center of the beam footprint) since it is inaccessible for RTD measurements. The figure shows that calculated temperatures are significantly higher at all flow values than those measured. The difference is greater at the *side* location (heater part), where air convection from the RTD's epoxy can be an important factor. All data in Fig. 4 (a) show that temperatures decrease with increasing flow, but at a lower rate at higher flows. An increase in the value of film coefficient, h_f , basically reduces the temperature rise across the film. The % reduction is essentially proportional to $(h_{f2} - h_{f1})/h_{f2}$ when the film coefficient is increased from h_{f1} to h_{f2} . A change in h_f has no significant impact on the temperature rise within the copper itself. At higher flows (equivalent to h_f of 1.5 W/cm²°C), the latter already dominates the total temperature rise, thereby reducing the benefit of further increase in flow.

(a)



(b)

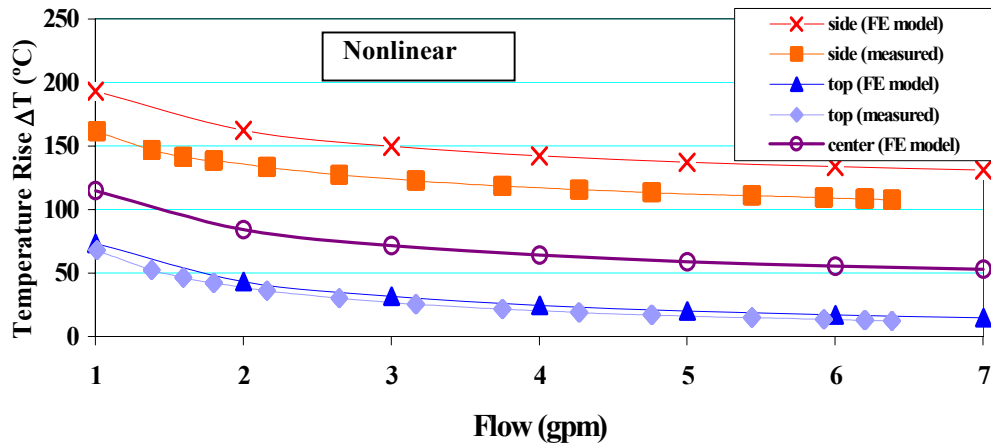


Fig. 4: Comparison of experimental and FE results for different flow values.
Effect of wall temperature on h_f ignored in (a) and included in (b).

Further FE analyses were performed including the effect of the viscosity factor (μ_b/μ_w) in Eq. (1). Even though this equation assumes a uniform wall temperature, we

used it as an approximation at each node of the cooling-channel perimeter. Since the channel wall temperatures were not known a priori, the FE results were obtained by using nonlinear solution option of ANSYS. These results, plotted in Fig. 4(b), show a better agreement with the experimental data, especially for the *top* location where the temperature rise decreased by 10-15%. Temperature-rise contours in the copper block for the case of 6-gpm flow are depicted in Fig. 5.

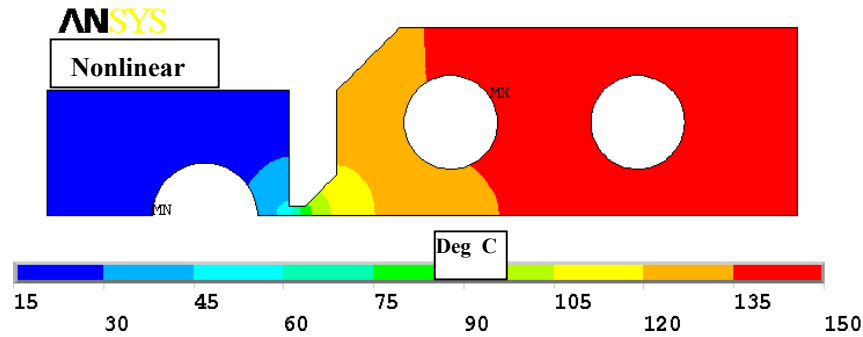
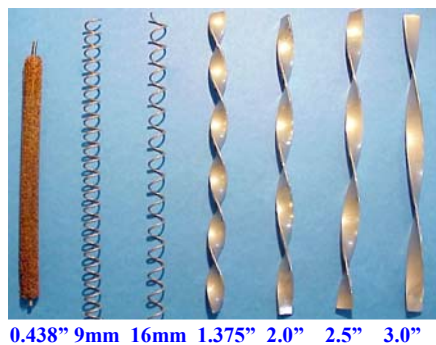


Fig. 5: Temperature-rise contours for the smooth-bore 6-gpm (nonlinear) case.

5. Experimental Results with Channel Inserts

Channel inserts used for the enhanced cooling consisted of an identical pair of 0.438" diameter copper wire mesh, 9 and 16 mm pitch springs of 1.4 mm wire thickness, and twisted tapes of 1.375", 2.0", 2.5" and 3.0" pitch (see Fig. 6). External diameters of the spring and twisted tapes were marginally larger than internal diameter of the water channel (0.438") such that insertions required a force-fit.



Channel Inserts

Fig. 6: Inserts for enhanced cooling.

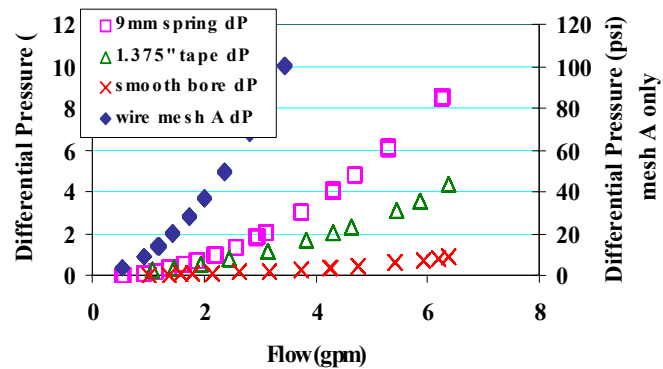


Fig. 7: Pressure drops (dPs) versus flow for various channel inserts.

The inserts require considerable higher pressure drops (dPs) for a given flow as compared to the smooth-bore channel. Figure 7 shows dPs versus flow for the smooth-bore wire mesh, 9-mm-pitch spring and 1.375"-pitch twisted tape. As expected, dP for the wire mesh is one order of magnitude higher than for the other inserts. For the 16-mm-

pitch spring, dP (not shown) was found to be essentially the same as that for the 9-mm-pitch spring. Similarly, while dP for the 2.0"-pitch tape was about 50% of that for the 1.375"-pitch tape, further decreases in dP for longer pitch tapes were not significant. This behavior, also evident for certain spring inserts used by Collins et al. [14], is not well understood.

Figure 8 shows plots of temperature rise versus flow curves for the different inserts. The wire-mesh inserts show high gain in enhanced cooling, Fig. 8(a). Their effective film coefficient at 1 gpm is about the same as that for the smooth-bore channel at 6 gpm ($1.5 \text{ W/cm}^2 \text{ }^\circ\text{C}$). Because of the high pressure drop, data for the wire-mesh inserts could be obtained only up to a flow of 3.5 gpm. In practical high-heat-load absorbers case, the flow would be limited to a 1-1.5 gpm range. Figure 8(b) compares smooth-bore data with that for the two spring inserts. Both the spring inserts show substantial but similar cooling enhancement with film coefficients at 2.5 gpm approaching $1.5 \text{ W/cm}^2 \text{ }^\circ\text{C}$. Results for the twisted-tape inserts are shown in Fig. 8(c). These inserts also show significant cooling enhancement, although, for a given flow, they are not as effective as the spring or wire-mesh inserts. The smaller pitch (1.375") twisted tape has the best performance, especially at lower flow, as compared to the other three longer-pitch tapes. This is consistent with the higher pressure drop for the 1.375"-pitch tape. All twisted tapes require about 4 gpm to achieve a film coefficient of $1.5 \text{ W/cm}^2 \text{ }^\circ\text{C}$. For an easy comparison, the best data for each type of inserts are plotted in Fig. 8(d) with that for the smooth-bore case.

6. Discussion

For given flow rates (in gpm), substantial improvements can be made in cooling efficiency by the wire-mesh, spring or twisted-tape inserts. Wire-mesh inserts show the best gains; however, past experience at the APS has shown that such inserts have a tendency to clog up even in high-purity water. Because of their high maintenance requirements in back flushing and flow monitoring, the wire-mesh inserts are no longer considered as an option in new designs.

While additional erosion-corrosion data are being collected for both the OFHC copper and Glidcop, the evidence at this point suggests no significant erosion-corrosion problem for up to 15 ft/sec of flow velocity (the design specification at LANL). This flow velocity yields a film coefficient, of greater than $1.5 \text{ W/cm}^2 \text{ }^\circ\text{C}$ for channel diameters of up to 0.5". The spring or twisted-tape inserts can easily achieve a film coefficient of up to

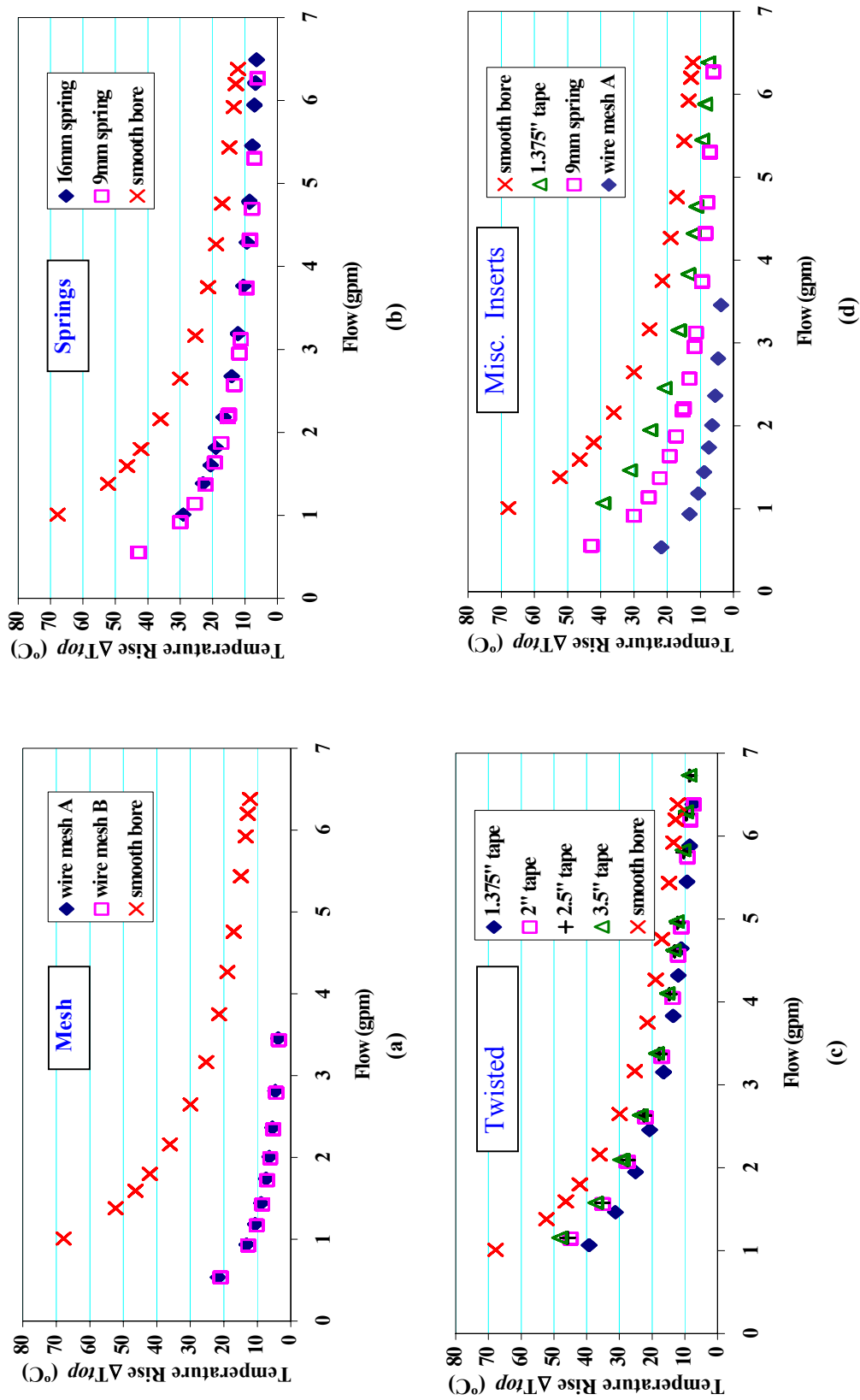


Fig. 8: Temperature rise, ΔT_{top} , versus flow for different types of channel inserts compared with the smooth-bore case. (a) Wire mesh, (b) springs, (c) twisted-tapes, and (d) selected inserts.

2.0 W/cm² °C at lower flow rates. Film coefficients greater than this value are generally not sought for two reasons: (1) their incremental advantage in lowering overall temperature rise is small (see Fig. 4), and (2) required flow rates are difficult to achieve because the available pressure drops are limited by header pressures. This is illustrated in Fig. 9, where temperature rise at the top location (ΔT_{top}) is plotted against pressure drop (dP) across the 6" copper channel. The smooth-bore data was measured only up to a flow of 6.4 gpm, which corresponded to a flow velocity of 13.6 ft/sec and a film coefficient of 1.5 W/cm² °C. For a ΔT_{top} reduction from 37 to 12°C, the smooth-bore has the lowest pressure drop, 0.8 psi, compared to about 2 psi for the spring or twisted-tape inserts. Further drop in ΔT_{top} is achievable by the channel inserts but at an exponentially rising pressure drop.

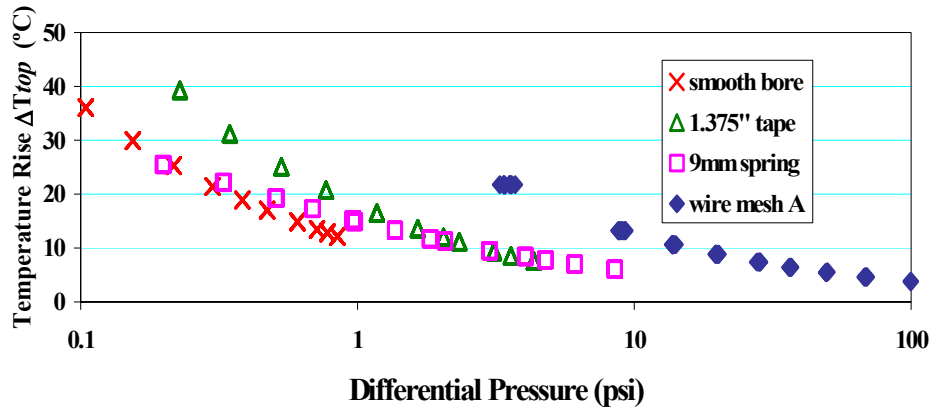


Fig. 9: Temperature versus differential pressure (dP) for selected inserts and the smooth-bore channel.

The gain from raising the film coefficient, h_f , from 1.5 to 2.0 W/cm² °C was estimated by the nonlinear FE model for an absorber application. Using the lower value, the heat load in the FE model was first increased to 7.0 kW to bring the channel wall temperature to 150°C, which is frequently used as a design criterion to avoid nucleate boiling. Temperatures are calculated again with the higher h_f value. Temperature rises at the *center* location (equivalent to the center of beam footprint) were 194.5°C and 172.9°C, respectively. The temperature rise was thus reduced by 21.6°C. Similar results have been obtained for a very complex geometry of a crotch absorber [1]. While this reduction in the temperature rise is only moderate, it would appear to come at no expense since the spring or twisted-tape inserts are inexpensive and easy to install. That would indeed be the case if no flow interlocks were implemented. Normally, high-heat-load components require flow-monitoring circuits at a significant (25-50%) fraction of the total cost. These circuits also require most of the maintenance effort and are susceptible to false trips. Several components with smaller dP requirements can be combined in one flow circuit to optimize cost and reliability. For instance, in the APS storage ring, each flow circuit contains two to four high-heat-load absorbers. Moreover, the channel inserts are difficult to use when complex flow paths are necessary (such as in the APS crotch absorber) for cooling optimization and for avoiding water-to-vacuum joints.

7. Conclusions

An evaluation of enhanced cooling techniques for high-heat-load absorbers has been presented. Based on available data and some erosion-corrosion test at the APS, a flow velocity of 15 ft/sec for copper and Glidcop channels in high-purity water is considered to be acceptable. This value corresponds to a film coefficient of at least 1.5 W/cm² °C in channels of less than 0.5" diameter. Experimental results for wire-mesh, spring and twisted-tape inserts have been presented showing significant improvement in cooling efficiency at lower flow rates. Only a moderate decrease in overall temperature rise is seen when the effective film coefficient is increased from 1.5 to 2.0 W/cm² °C by using such channel inserts. The use of channel inserts can, however, limit design choices and result in significant increase in the cost and maintenance of flow instrumentation.

8. Acknowledgments

The Authors would like to thank K. Boerste, M. Bracken, H. DeLeon, C. Putnam, and B. Rusthoven for various technical assistance, and C. Eyberger and K. Jaje for editing this paper. This work was supported by the U.S. Department of Energy under Contract No. W-31-109-ENG-38.

9. References

- [1] A. Alp, "Thermal Stress Analysis of High-Heat-Load Crotch Absorbers at the APS," these proceedings.
- [2] Y. Jaski, "Thermo-mechanical Analysis of High-Heat-Load Components for the Canted Undulator Beamlines," these proceedings.
- [3] T.M. Kuzay, J.T. Collins, A.M. Khounsary and M. Gilberto, "Enhanced Heat Transfer with Wool-Filled Tubes," ASME/JSME 3rd Joint Heat Engineering Conference, Reno, Nevada, March 1991.
- [4] R.M. Manglik and BERGLES, A.E., "Heat Transfer and Pressure Drop Correlations for Twisted-Tape Inserts in Isothermal Tubes: Part I, Laminar Flows," Journal of Heat Transfer, Vol. 115, pp. 881-889 (1993).
- [5] T. Takia, T. Mochizuki and H. Kitamura, "Development of Enhanced Heat Transfer Coolant Channels for the SPring-8 Front End Components," Spring-8 Annual Report, 1998, pp. 164-166.
- [6] <http://www.copper.org/tubehdbk/design-data-pressure.html>
- [7] <http://www.ccbda.org/publications/is-97-02-publication-e.html>
- [8] D. Schrage, Los Alamos National Laboratory, New Mexico, e-mail communication, August 2002.
- [9] D. Lynch, Brookhaven National Laboratory, New York, e-mail communication, August, 2002.
- [10] GlidCop; "Copper Dispersion Strengthened with Aluminum Oxide," SCM Metal Products, Inc 1994.
- [11] R. L. Dobson and J. B. Whitley, "Erosion-Corrosion of Copper in a High Velocity Water Environment," Report No. SAND-87-0312, Sandia National Laboratories, Albuquerque, New Mexico, 1987.

- [12] R.H. Perry and C. H. Chilton, (editors) Chemical Engineers' Handbook, 6th ed., McGraw-Hill, 1984.
- [13] Welty J., Wicks C., and Wilson R., Fundamentals of Momentum, Heat, and Mass Transfer, 3rd. Edition, Wiley & Sons Inc., 1984.
- [14] J.T. Collins, C.M. Conley, J.N. Attig and M.M. Baehl, "Enhanced Heat Transfer Utilizing Wire-Coil Inserts for High-Heat-Load Applications," these proceedings.